ACS APPLIED MATERIALS & INTERFACES

Research Article

www.acsami.org

Engineered Therapeutic-Releasing Nanoporous Anodic Alumina-Aluminum Wires with Extended Release of Therapeutics

Cheryl Suwen Law,[†] Abel Santos,*[,†] Tushar Kumeria,[†] and Dusan Losic*[,†]

[†]School of Chemical Engineering, The University of Adelaide, Adelaide, SA 5005, Australia

Supporting Information

ABSTRACT: In this study, we present a nanoengineered therapeutic-releasing system based on aluminum wires featuring nanoporous anodic alumina layers and chitosan coatings. Nanoporous anodic alumina layers are produced on the surface of aluminum wires by electrochemical anodization. These nanoporous layers with precisely engineered nanopore geometry are used as nanocontainers for bovine serum albumin molecules labeled with fluorescein isothiocyanate (BSA-FITC), which is selected as a model drug. The surface of these therapeutic-releasing implants is coated with a biocompatible and biodegradable polymer, chitosan, in order to achieve a sustained release of protein over extended periods of time. The performance of this therapeutic-releasing device is systematically assessed through a series of experiments under static and dynamic flow conditions. In these experiments, the effect of such parameters as the number of layers of chitosan coating and the temperature and pH of the eluting medium is established. The obtained results reveal that the proposed therapeutic-releasing system based on nanoporous aluminum wires can be engineered with sustained release performance for up to 6.5 weeks, which is a critical factor for medical treatments using sensitive therapeutics such as proteins and genes when a localized delivery is desired.

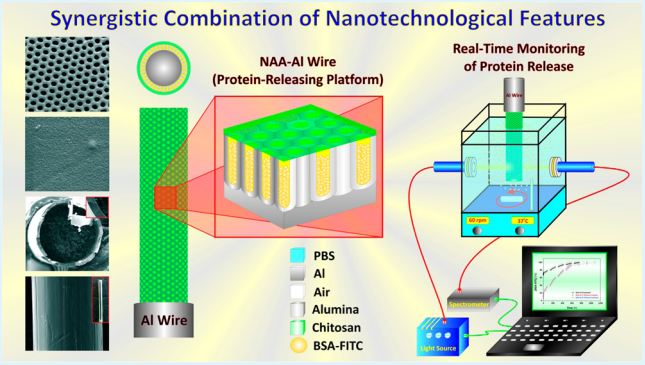

KEYWORDS: *aluminum wires, therapeutic release, nanoporous anodic alumina, chitosan coatings, simulated body conditions*

1. INTRODUCTION

Therapeutic implantable delivery systems are recognized as a promising alternative to conventional clinical treatments based on systemic administration of therapeutics via oral or intravenous routes, which present some inherent limitations of such as the peak-and-valley effect, toxicity, biodegradability, poor biodistribution, retention in natural barriers, bioavailability, selectivity, and adverse pharmacokinetics and pharmacodynamics.[1−4] Implantable therapeutic-releasing systems can provide a precise control over the dosage of therapeutics, keeping their levels at the site of action within the therapeutic window throughout. This makes therapies more efficient and effective, since less amount of therapeutics is required, and less aggressive, given that side effects associated with overdose of toxic therapeutics can be overcome.[5−9] Pioneering implantable releasing systems were based on hormone pellets, which were aimed to improve the growth of livestock.[10] These systems were subsequently used in clinical therapies based on the administration of hormones to young women suffering from premature menopause.[11] More recently, nanotechnological approaches have made it possible to develop highly sophisticated releasing systems for a broad range therapeutics.[3] These systems, which can be produced with state-of-the-art and cutting edge technical features, have demonstrated outstanding versatility for releasing multiple therapeutics in a localized manner, overcoming the inherent limitations of conventional therapies and making treatments more effective and efficient.

Regardless of the many advantages associated with implantable releasing systems, these medical devices have some drawbacks. As an example, in many cases, these systems require invasive surgery to be implanted, limiting their applicability for treating diseases affecting difficult-to-access organs such as brain or bones.[12] Recently, some nanotechnological approaches have enabled the development of miniaturized therapeutic-releasing systems, which can be implanted by means of minimal surgery and release therapeutics over difficult-to-access organs. In particular, titanium (Ti) wires featuring layers of titanium nanotubes (TNTs) have been envisaged as an alternative system to treat cancers affecting brain and bones.[13−15] TNTs fabricated by electrochemical anodization of Ti substrates with different shapes (e.g., foils, wires, stents, screws, etc.) can be produced with well-controlled geometry and surface chemistry.[16] TNTs-Ti implants have been extensively researched during the last years as therapeutic-releasing platforms for localized drug delivery applications and potential treatment of bone-,

Received: December 30, 2014
Accepted: January 27, 2015
Published: January 27, 2015

DOI: 10.1021/am5091963
ACS Appl. Mater. Interfaces 2015, 7, 3846−3853

cardiovascular- and cancer-related diseases.[17−20] Furthermore, TNTs have demonstrated good biocompatibility, biointegration and capability to release therapeutics in a controlled manner. However, it is worthwhile noting that TNTs layers grown on Ti have poor mechanical strength and stability, which are critical properties required for implants subjected to significant mechanical stress. In addition, TNTs layers grown on curved Ti surfaces present cracks produced by the volume expansion oxide-metal, which takes place during anodization. These cracks weaken TNTs layers, which are susceptible to peel off from the underlying Ti substrate under mechanical stress.[21] Recent in vivo studies with porcine models have shown that the shedding of particle debris released from inorganic layers grown on the surface of implantable medical devices can lead to inflammation of surrounding tissues and fatal failure and rejection of the implant.[22] In that respect, it has been demonstrated that nanoporous structures are more compact and present better mechanical robustness, adhesion, and stability than nanotubular structures.[21] Therefore, inert inorganic materials such as nanoporous anodic alumina (NAA) are considered as a promising alternative to TNTs-Ti releasing systems.[3] NAA is produced by electrochemical anodization of aluminum (Al) substrates.[23−28] The resulting nanoporous films present excellent mechanical properties and adhesion to the underlying Al substrate, versatility in terms of pore geometry and surface chemistry, good biocompatibility and biostability, and negligible leakage of aluminum ions.[3,29−32] Previous studies have extensively explored the use of NAA-based structures as nanoporous matrix to release therapeutics for potential medical applications.[4,33] Nevertheless, to the best of our knowledge, so far wirelike NAA-Al structures have not been explored as a potential alternative to therapeutic-releasing platforms based on TNTs-Ti wires.

In this context, we develop and assess for the first time an implantable nanoengineered therapeutic-releasing device based on NAA-Al wires with sustained and extended release of therapeutics for up to several weeks. Figure 1 illustrates the proposed therapeutic-releasing system combining NAA-Al wires with chitosan coatings. NAA layers with precisely controlled nanopore geometry are produced on the surface of aluminum wires by electrochemical anodization. The resulting nanopores are subsequently used as nanocontainers for a model protein, bovine serum albumin labeled with fluorescein isothiocyanate (BSA-FITC). Chitosan coatings of different thicknesses are incorporated into this system on the top surface of NAA nanopores as a means of extending the release of protein over longer periods of time. The release characteristics of the proposed therapeutic-releasing system are engineered by the geometric features of NAA nanopores (i.e., pore diameter and its length) and the thickness and degradation of chitosan coatings. The performance of this device is systematically assessed through a series of experiments under static and dynamic conditions, by which the effects of the number of layers of chitosan coating and the temperature and pH of the eluting medium on the release performance are established. Note that, in the context of this study, dynamic flow conditions are specifically applied in order to mimic the actual conditions of implants, where surrounding physiological fluids flow continuously around the implant. This has a considerable impact on the release of therapeutics from the implant as compared to static conditions, where the eluting medium remains stagnant throughout.

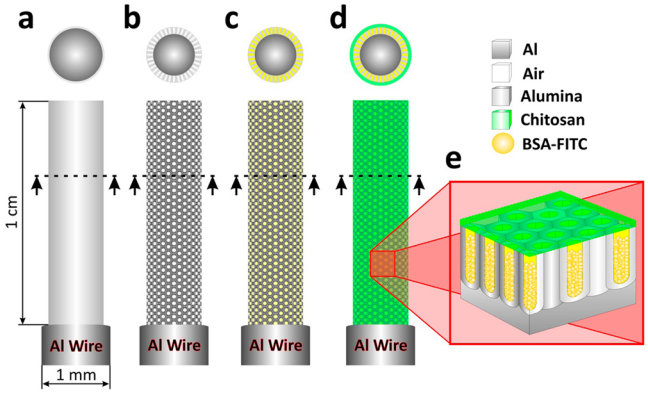

Figure 1. Scheme of therapeutic-releasing NAA-Al wires combining NAA layers and chitosan coatings. (a) Al wire after electropolishing. (b) NAA-Al wire after two-step anodization. (c) NAA-Al wire after protein (BSA-FITC) loading. (d) Protein-loaded NAA-Al wire after application of chitosan coating. (e) Magnified view of the proposed system for releasing therapeutics.

2. EXPERIMENTAL SECTION

2.1. Materials. Al wires of 1 mm in diameter and purity 99.9997% were supplied by Goodfellow Cambridge Ltd. (UK). Oxalic acid ($C_2H_2O_4$), phosphoric acid (H_3PO_4), hydrochloric acid (HCl), perchloric acid ($HClO_4$), acetic acid ($C_2H_4O_2$), chromium trioxide (CrO_3), ethanol (C_2H_5OH), copper(II) chloride ($CuCl_2$), bovine serum albumin fluorescein isothiocyanate conjugate (BSA-FITC), chitosan low molecular weight, and phosphate buffered saline (PBS) were obtained from Sigma-Aldrich (Australia) and used as received without further purification steps. All the solutions used in this study were prepared with ultrapure water Option Q−Purelabs (Australia).

2.2. Fabrication of NAA-Al Wires. Anodization of high-purity Al wires by a two-step anodization process yielded nanoporous anodic alumina layers on the surface of Al wires.[23−28] In this process, Al wires 10 cm long and 1 mm in diameter were sonicated in ethanol (EtOH) and distilled water for 15 min each and dried under nitrogen stream. Al wires were wrapped with Teflon tape so that only 1 cm of wire was exposed the acid electrolyte. Then, Al wires were electropolished in a mixture of EtOH and $HClO_4$ 4:1 (v:v) at 20 V and 5 °C for 1 min. Subsequently, the first anodization step was carried out in an aqueous solution 0.3 M $H_2C_2O_4$ at 40 V and 6 °C for 20 h. The resulting NAA layer with disordered nanopores on its top was chemically removed by wet chemical etching in a mixture of 0.4 M H_3PO_4 and 0.2 M chromic acid (H_2CrO_4) at 70 °C for 3 h. Next, the second anodization step was performed using the same acid electrolyte at 6 °C for 20 h. Finally, the nanoporous structure was widened by wet chemical etching in H_3PO_4 5 wt % at 35 °C for 15 min in order to increase the loading capacity of NAA for BSA-FITC molecules. Note that the remaining aluminum substrate was removed by chemical etching in a mixture of $HCl/CuCl_2$ in order to obtain cross-section images of the resulting NAA layers.

2.3. Protein Loading. One mg mL^{-1} stock solution of BSA-FITC was prepared in PBS at pH 7.5. NAA layers produced on the surface of Al wires were loaded with BSA-FITC molecules by vacuum-assisted infiltration. In this process, Al wires were immersed in the stock solution of FITC-BSA for 5 min under vacuum in order to expel any air bubbles trapped in the nanopores and to facilitate the loading of protein molecules. Then, protein-loaded NAA-Al wires were dried at 45 °C for 30 min. Note that a mild temperature and a short drying time were selected in order to prevent protein molecules from degradation. The loading and drying steps were repeated 5 times each in order to achieve an optimal protein loading. The total amount of protein loaded per NAA-Al wire was established by thermogravimetric analysis (TGA) (TGA Q500 V20.13 Build 39, TA Instruments, USA) (see Figure S1 in the Supporting Information).[34,35]

DOI: 10.1021/am5091963
ACS Appl. Mater. Interfaces 2015, 7, 3846−3853

2.4. Chitosan Coatings on Protein-Loaded NAA-Al Wires. Protein-loaded NAA-Al wires were coated with chitosan layers of controlled thickness by dip coating process. To this end, we used a custom-built dip coating system, in which NAA-Al wires were dipped into an aqueous solution of chitosan (1 wt/v % chitosan in 0.8 *v* % of acetic acid) at a controlled rate of 1 mm min^{-1}, which was maintained by a syringe pump (Fusion 200 Touch series, Chemyx Inc., USA). After each coating cycle (i.e., infusion and withdrawn modes), the remaining solvent was evaporated from the resulting chitosan film at 45 °C for 30 min. In this study, we analyze the release of protein from NAA-Al wires featuring chitosan coatings produced by 1 and 5 coating cycles.

2.5. Assessment of In Vitro Protein Release under Static and Dynamic Conditions. The protein release performance of chitosan-coated NAA-Al wires was assessed through a series of in vitro experiments carried out under static (i.e., without stirring) and dynamic (i.e., with stirring) conditions. As far as experiments performed under static conditions is concerned, chitosan-coated protein-loaded NAA-Al wires were dipped into 3 mL of PBS solution at 20 °C and pH 7.5. 0.5 mL of eluting medium was pipetted at established periods of time (i.e., every 15 min during the first hour, every 30 min for the second hour, every hour for the next 4 h and finally every 24 h) (Figure 2a). Note that the volume of eluting

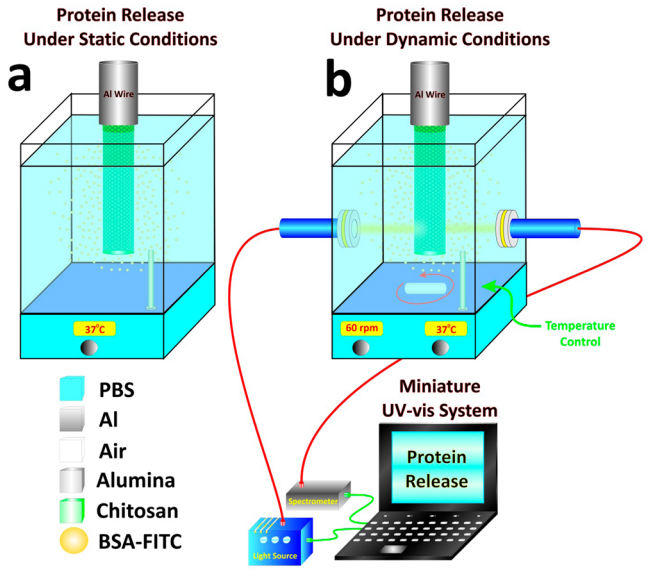

Figure 2. Scheme of the experimental setups used to assess the release performance of therapeutic-releasing Al wires with NAA layers and chitosan coatings. (a) Experimental setup for static flow conditions. (b) Experimental setup for dynamic flow conditions.

medium pipetted in each of the aforementioned steps was replaced by the same volume of fresh PBS solution in order to keep the system under perfect sink conditions.[36] The amount of protein released with time was established by a fluorescence spectrometer (Fluoromax-4, Horiba Jobin Yvon) equipped with a Xe lamp at room temperature used as excitation light source. The excitation wavelength (λ_{ex}) was set to 495 nm with a slit size of 5 nm and the emission intensity from BSA-FITC molecules was measured at 566 nm (λ_{em}). A calibration curve was used to establish a direct relationship between fluorescence intensity and protein concentration (see Figure S2 in the Supporting Information). In-vitro protein release studies under dynamic conditions were carried out by immersing the active tip of chitosan-coated NAA-Al wires in a cuvette containing 3 mL of PBS solution at 20 °C and pH 7.5. This system was placed on a magnetic stirrer (IKA Labortechnik RTC basic – ETS-D4 Fuzzy) and a miniature magnetic bar (i.e., 0.5 mm in diameter and 2 mm in length) was used to stir the eluting medium at a constant rate of 60 r.p.m. throughout. This setup was designed to mimick dynamic flow conditions present in real in vivo scenarios (Figure 2b). A miniature optical fiber UV–visible spectrometer (USB2000+VIS-NIR-ES, Ocean Optics, USA) was used to measure the absorbance of BSA-FITC molecules (λ_{abs} = 495 nm) released from the NAA-Al wires into the eluting medium in real-time. A calibration curve was used to establish a direct relationship between absorbance and protein concentration in the eluting medium (see Figure S2 in the Supporting Information). Note that 0.5 mL of eluting medium was replaced by the same volume of fresh PBS solution every 12 h in order to keep the system under perfect sink conditions.

2.5.1. Effect of Chitosan Coatings on Protein Release from NAA-Al Wires. The effect of chitosan coatings on the protein release performance from BSA-FITC-loaded NAA-Al wires was assessed under static and dynamic conditions. To this end, we studied the in vitro release of protein from (i) protein-loaded NAA-Al wires without chitosan coating (i.e., control), (ii) protein-loaded NAA-Al wires with 1 chitosan coating, and (iii) protein-loaded NAA-Al wires with 5 chitosan coatings. The eluting medium in these experiments was PBS at 20 °C and pH 7.5.

2.5.2. Effect of Eluting Medium Temperature on Protein Release from NAA-Al Wires. The effect of the eluting medium temperature on the protein release from BSA-FITC-loaded NAA-Al wires was assessed under static and dynamic conditions. As far as the former set of experiments is concerned, a water bath was used to keep the eluting medium temperature at 37 °C throughout. As mentioned above, 0.5 mL of eluting medium was pipetted at different time intervals and replaced with fresh PBS at controlled temperature. Finally, the amount of BSA-FITC released was established by fluorescence (vide supra). To analyze the effect of the eluting medium temperature on the in vitro protein release performance under dynamic conditions, the temperature of the eluting medium was kept at 37 °C throughout by a hot plate equipped with magnetic stirrer and temperature probe. Absorbance of the eluting medium was monitored in real-time by the aforementioned optical system until the total amount of BSA-FITC was released. Note that in these experiments, the eluting medium was PBS at pH 7.5 and protein-loaded NAA-Al wires with 5 chitosan coatings were used. Furthermore, vials and cuvettes were properly sealed in order to avoid evaporation of the eluting medium in the course of these experiments.

2.5.3. Effect of Eluting Medium pH on Protein Release from NAA-Al Wires. The effect of the pH of the eluting medium on the protein release performance from chitosan-coated NAA-Al wires under static and dynamic conditions was studied by adjusting the pH of PBS to 5.5. In these experiments, protein-loaded NAA-Al wires with 5 chitosan coatings were used and the temperature of the eluting medium was set to 20 °C throughout.

2.6. Structural Characterization of NAA-Al Wires. The structural features of NAA-Al wires after each fabrication step were characterized by SEM images acquired by field emission gun scanning electron microscopy (FEG-SEM FEI Quanta 450). NAA-Al wires were cut into small pieces of approximately 1.5 cm and subsequently mounted on a holder using conductive carbon tape. These samples were then coated with a thin layer of platinum (5 nm, approximately). Reflectometric interference spectroscopy (RIfS) was used to establish the thickness of chitosan coatings on the surface of NAA-Al wires after dip coating process (see Figure S3 in the Supporting Information).

Note that all the aforementioned experiments were repeated three times using freshly prepared NAA-Al wires.

RESULTS AND DISCUSSION

3.1. Structural Characterization of Chitosan-Coated NAA-Al Wires. The morphology of the resulting NAA-Al wires after each fabrication step (i.e., bare Al wire, electropolished Al wire, NAA-Al wire after first anodization step, Al wire after NAA removal, NAA-Al wire after second anodization step, NAA-Al wire after pore widening and NAA-Al wire after chitosan coating) was characterized by SEM images (see Figure S4 in the Supporting Information). Figure 3 shows a set of representative SEM images of a NAA-Al wire after second anodization, pore widening and chitosan coating processes,

DOI: 10.1021/am5091963
ACS Appl. Mater. Interfaces 2015, 7, 3846–3853

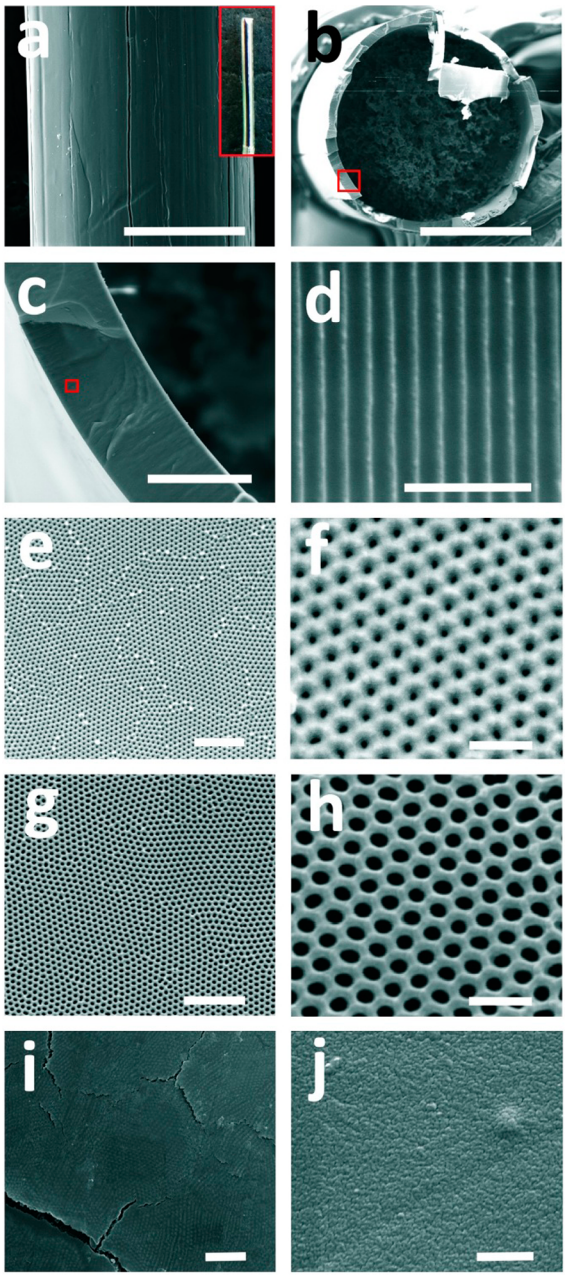

Figure 3. Set of SEM images of NAA-Al wires after different fabrication stages. (a) General view of NAA-Al wire after second anodization step (scale bar = 500 μm); inset shows a digital image of the resulting NAA-Al wire. (b) General cross-section view of NAA-Al wire after second anodization step (scale bar = 500 μm); note that the underlaying aluminum substrate was partially dissolved for imaging purposes. (c) Magnified view of red square shown in b (scale bar = 50 μm). (d) Magnified view of red square shown in c with details of NAA nanopores (scale bar = 500 nm). (e) Top view of NAA-Al wire after second anodization step (scale bar = 1 μm). (f) Magnified view of e (scale bar = 250 nm). (g) Top view of NAA-Al wire after pore widening (H_3PO_4 5 wt % at 35 °C) (scale bar = 1 μm). (h) Magnified view of (g) (scale bar = 250 nm). (i) Top view of NAA-Al wire after chitosan coating (1 coating cycle) (scale bar = 1 μm). (j) Top view of NAA-Al wire after chitosan coating (5 coating cycles) (scale bar = 1 μm).

respectively. Likewise, in flat Al substrates, a two-step anodization process yields NAA layers featuring hexagonally arranged arrays of cylindrical nanopores across the surface of the Al wire (Figures 3a–d).[23−28] The geometric features of the resulting NAA layers (i.e., interpore distance (d_{int}), pore diameter (d_p), and length (L_p)) were established by SEM image analysis. The obtained results revealed an average d_p of 35 ± 2 nm and 50 ± 4 nm before and after pore widening (i.e., 15 min), respectively, an average L_p of 62 ± 1 μm and an average d_{int} of 102 ± 5 nm (Figures 3e–h). These results are in good agreement with previously reported values of geometric features of nanopores in NAA produced on flat Al substrates under the same anodization conditions.[28] This result is reasonable given that NAA nanopores grow perpendicularly to the surface of the underlying aluminum substrate, independently of its geometry.[28] Note that BSA-FITC is a big protein molecule with a molecular weight of 66.5 kDa and a Stokes radius of 3.5 nm.[37] Therefore, NAA nanopores were widened by wet chemical etching in order to facilitate the infiltration of BSA-FITC molecules and increase the amount of protein loaded in each NAA-Al wire.[4] Thermogravimetric analysis established that the average total amount of protein loaded in each NAA-Al wire (i.e., 1 cm long and 0.9 mm in diameter, approximately) was 0.185 ± 0.020 mg of BSA-FITC per NAA-Al wire (see Figure S1 in the Supporting Information).

After protein infiltration, NAA-Al wires were coated with chitosan films of controlled thickness by dip coating approach. Figures 3i, j show top-view SEM images of NAA-Al wires coated with chitosan after 1 and 5 coating cycles, respectively. These images reveal that whereas chitosan films produced by 1 coating cycle presented cracks, films produced by 5 coating cycles coated the surface of NAA-Al wires homogeneously and no cracks were observed. It is worthwhile noting that the homogeneity of the chitosan film is a critical factor to control and extend the release of protein. The thickness of the resulting chitosan coatings were established by RIfS using flat NAA-Al substrates with chitosan coatings produced under the same conditions than those used for NAA-Al wires (Figure S3 in the Supporting Information). RIfS is an optical technique based on the constructive interference of white light with thin films, the physical thickness of which can be optically estimated from the effective optical thickness.[38−41] The obtained results established that chitosan films produced by 1 and 5 coating cycles presented an average thickness of 2.1 ± 0.2 μm and 10.7 ± 0.3 μm, respectively.

3.2. In Vitro Protein Release from NAA-Al Wires under Static Conditions. As mentioned above, the in vitro protein release performance of NAA-Al wires under static conditions was characterized by measuring the fluorescence intensity of aliquots pipetted at fixed periods of time. Table 1 summarizes the results obtained from this set of experiments. Figure 4a shows the release of protein from NAA-Al wires without chitosan coating and with 1 and 5 cycles of chitosan coatings. At first glance, it is observed that uncoated NAA-Al wires present a considerable initial burst release stage during the first 6 h of release, where nearly 75% of the loaded protein is released. This behavior, which is in good agreement with previous studies, is due to free diffusion of BSA-FITC molecules driven by the high gradient of protein concentration between the eluting medium and nanopores.[5−9] The application of chitosan coatings on the surface of therapeutic-releasing NAA-Al wires significantly minimizes the initial burst release to 20%, approximately. Note that a small amount of protein is expected to be released during the initial stage after first contact with the buffer solution since some BSA-FITC

DOI: 10.1021/am5091963
ACS Appl. Mater. Interfaces 2015, 7, 3846−3853

Table 1. Summary of Effects of Chitosan Coating and pH and Temperature of Eluting Medium on the Release Performance of Protein-Loaded NAA-Al Wires under Static Conditions

flow conditions	parameter analyzed	label	release time (h)
static	chitosan coating	NAA-Al (uncoated)	751
		NAA-Al (1 chitosan coating)	917
		NAA-Al (5 chitosan coating)	1088
	pH	NAA-Al (pH 7.5)	1088
		NAA-Al (pH 5.5)	650
	temperature	NAA-Al (T = 20 °C)	1088
		NAA-Al (T = 37 °C)	773

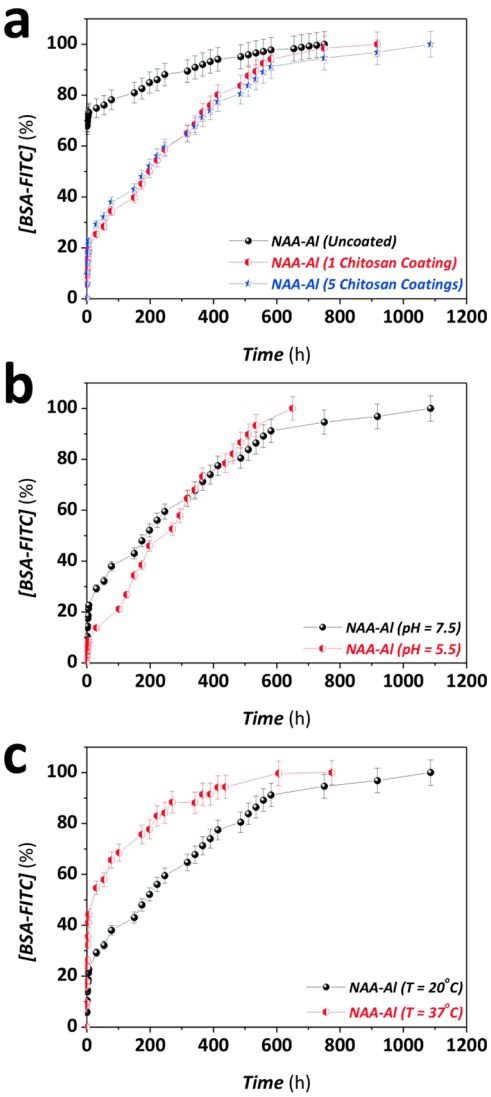

Figure 4. Protein release performance from chitosan-coated NAA-Al wires under static conditions. (a) Effect of chitosan coatings on the release performance of NAA-Al wires (eluting medium PBS at 20 °C and pH 7.5). (b) Effect of pH on the release performance of NAA-Al wires (NAA-Al wire with 5 chitosan coatings and eluting medium PBS at 20 °C). (c) Effect of temperature on the release performance of NAA-Al wires (NAA-Al wire with 5 chitosan coatings and eluting medium PBS at pH 7.5).

molecules are incorporated on the surface of the chitosan coating during the coating process. More significant differences between uncoated and coated NAA-Al wires were observed in the second stage of release (Figure 4a). As Table 1 shows, chitosan coatings enabled an extended release of therapeutic protein from 751 h to 917 and 1088 h for NAA-Al wires with 1 and 5 chitosan coatings, respectively. The sustained release provided by chitosan-coated NAA-Al wires (i.e., up to 6.5 weeks) is significant for this type of therapeutic-releasing devices, demonstrating their excellent potential as an alternative implant platform, when a long and sustained release of therapeutics is required. Furthermore, the therapeutic-releasing behavior after the incorporation of chitosan coatings denotes a zero order kinetics, which is desired for therapies based on localized delivery of therapeutics. This analysis verifies that the therapeutic-releasing performance is influenced by the number of chitosan coatings and the thicker the chitosan coating the more sustained the release of protein, which is in good agreement with previously reported studies on drug-releasing systems based on TNTs-Ti.[42] Note that BSA-FITC molecules must diffuse through the chitosan coating before they are released into the eluting medium. Therefore, this process hinders, retards, sustains, and extends the release of protein molecules over time as compared to uncoated NAA-Al wires. Chitosan is a water-soluble hydrophilic polymer and thus undergo chemical degradation in PBS. The dissolution of chitosan enhances the diffusion of BSA-FITC molecules from the nanopores to the eluting medium with time, as the coating degrades. Another factor affecting the release of protein molecules through the chitosan coatings is the presence of cracks and defects. As commented above, chitosan coatings produced on the surface of NAA-Al wires by a single coating cycle presented cracks and defects, which can act as preferential paths through which BSA-FITC molecules can diffuse directly from the nanopores to the eluting medium without impediment. Therefore, the resulting therapeutic-releasing behavior of chitosan-coated NAA-Al wires results from a combination of two factors, namely (i) degradation of chitosan coating and (ii) diffusion of BSA-FITC molecules from the nanopores to the eluting medium.

To gain insight into other factors affecting the release of protein from chitosan-coated NAA-Al wires, we studied the performance of the proposed system under acidic eluting medium. This aspect of our study is important for potential localized treatment of cancer as physiological fluids in cancerous tissues are known to be slightly acidic. To this end, the pH of PBS was adjusted to 5.5, which is lower than the pK_a of chitosan (i.e., 6.3), and the release of BSA-FITC molecules from NAA-Al wires with 5 chitosan coatings was studied (Figure 4b). The obtained results reveal that the release of protein is faster at pH 5.5 (650 h). It is worth stressing that the solubility of chitosan increases at pH 5.5, resulting in an increased degradation rate of chitosan and thus in a faster diffusion of BSA-FITC molecules through the chitosan coating.[43]

Another set of experiments under static conditions was designed to mimic the physiological conditions at the implant site in the host body. These experiments were carried out by keeping the temperature of the eluting medium at 37 °C. In these experiments, the release performance of protein-loaded NAA-Al wires with 5 cycles of chitosan coatings was assessed in PBS at pH 7.5 and 20 and 37 °C (Figure 4c). The obtained results revealed that the higher the temperature the faster the

DOI: 10.1021/am5091963
ACS Appl. Mater. Interfaces 2015, 7, 3846−3853

release of protein molecules from chitosan-coated NAA-Al wires. The increment of the eluting medium temperature accelerates the release of protein molecules (773 h) by degrading the chitosan coating at a faster rate and by enhancing the diffusion rate constant of BSA-FITC molecules from the nanopores to the eluting medium.[44]

3.3. In Vitro Protein Release from NAA-Al Wires under Dynamic Conditions. Typically, the release performance of therapeutic-releasing systems is characterized using different techniques under static conditions. However, as previous studies have demonstrated, these conditions are far from real in vivo conditions, in which surrounding body fluids flow around the surface of implants.[34] Ex vivo systems make it possible to mimic in vivo conditions closely and thus design and engineer releasing systems with more optimal capabilities. Nevertheless, these systems are expensive and sample preparation is laborious and complicated given that cells/tissues/organs must be kept in good conditions throughout the course of the experiments.[4,14] Although far from in vivo or ex vivo models, dynamic in vitro conditions can provide more accurate information on the release performance of therapeutic-releasing systems than traditional static in vitro conditions, making it possible to achieve a better understanding of different phenomena taking place in these processes. In this study, we characterized the performance of the proposed therapeutic-releasing NAA-Al wires under dynamic in vitro conditions in order to gain a more realistic insight into the capabilities of this system for real-life applications.

The in vitro protein release performance from NAA-Al wires under dynamic conditions was characterized by measuring the UV−visible absorbance of the eluting medium in real-time as indicated in the Experimental Section (vide supra). The obtained results are summarized in Table 2. Figure 5a depicts

Table 2. Summary of Effects of Chitosan Coating and pH and Temperature of Eluting Medium on the Release Performance of Protein-Loaded NAA-Al Wires under Dynamic Conditions

flow conditions	parameter analyzed	label	release time (h)
dynamic	chitosan coating	NAA-Al (uncoated)	14
		NAA-Al (1 chitosan coating)	19
		NAA-Al (5 chitosan coating)	65
	pH	NAA-Al (pH 7.5)	65
		NAA-Al (pH 5.5)	7
	temperature	NAA-Al (T = 20 °C)	65
		NAA-Al (T = 37 °C)	35

the release of BSA-FITC molecules from NAA-Al wires without chitosan coating and with 1 and 5 cycles of chitosan coatings under dynamic flow conditions in PBS at pH 7.5 and 20 °C. These results show that protein is released at a faster rate from uncoated NAA-Al wires (14 h). The application of 1 and 5 chitosan coatings on the surface of therapeutic-releasing NAA-Al wires sustains the release of BSA-FITC molecules throughout time and the higher the number of chitosan coatings the longer the release of protein (19 and 65 h, respectively). As compared to experiments performed under static flow conditions, the release of protein is much faster in all the cases because the dynamic flow of eluting medium around NAA-Al wires increases the diffusion rate of protein molecules

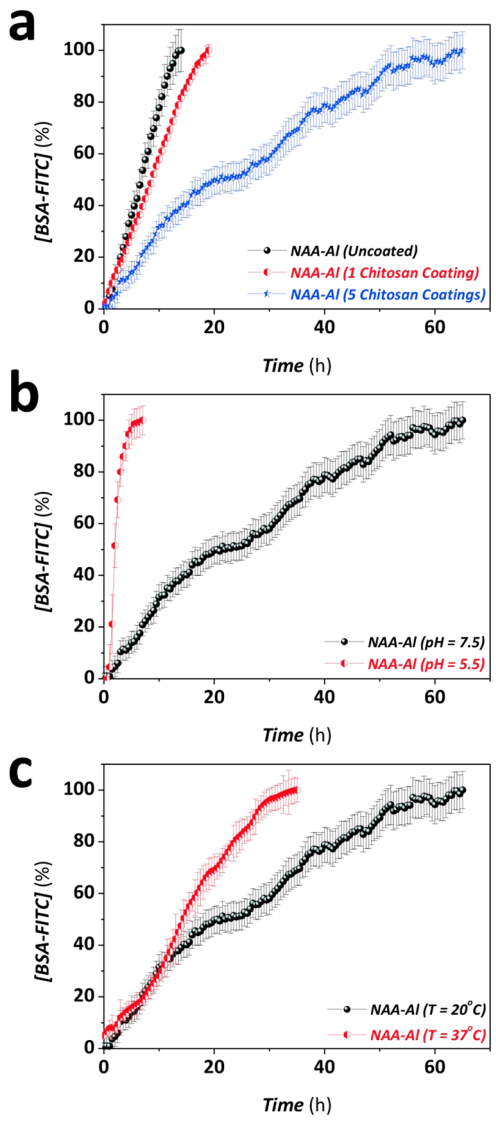

Figure 5. Protein release performance from chitosan-coated NAA-Al wires under dynamic conditions. (a) Effect of chitosan coatings on the release performance of NAA-Al wires (eluting medium PBS at 20 °C and pH 7.5). (b) Effect of pH on the release performance of NAA-Al wires (NAA-Al wire with 5 chitosan coatings and eluting medium PBS at 20 °C). (c) Effect of temperature on the release performance of NAA-Al wires (NAA-Al wire with 5 chitosan coatings and eluting medium PBS at pH 7.5).

from the nanopores to the eluting medium and chitosan degrades at a faster rate by the action of PBS. Another interesting result observed in these experiments is that the effect of the number of chitosan coating cycles is more marked under dynamic flow conditions, probably due to the degradation mechanism of chitosan under these conditions.

To obtain a better understanding of the effect of the pH and temperature of the eluting medium on the release performance of NAA-Al wires, we assessed the impact of these parameters under dynamic flow conditions as well. Figure 5b shows the effect of the pH of the eluting medium on the release of BSA-FITC molecules from NAA-Al wires with 5 chitosan coatings at 20 °C. The obtained results denote that BSA-FITC molecules are released faster at pH 5.5 (7 h) than at pH 7.5 (65 h). Again, it is observed that the effect of pH is much more marked under dynamic flow conditions than under static conditions. As far as

DOI: 10.1021/am5091963
ACS Appl. Mater. Interfaces 2015, 7, 3846−3853

the effect of the eluting medium temperature is concerned, Figure 5c illustrates the protein release characteristic from NAA-Al wires with 5 chitosan coatings at pH 7.5 and 20 and 37 °C. Again, it is observed that protein is released at a faster rate when the temperature of the eluting medium is increased (35 h).

3.4. Comparison of in Vitro Protein Release from NAA-Al Wires under Static and Dynamic Conditions. As the above-shown results demonstrate, the release performance of protein molecules from NAA-Al wires under static and dynamic flow conditions is affected in a similar way by the different parameters analyzed in this study (i.e., increment of chitosan coating thickness and pH and temperature of the eluting medium). It was observed that the use of chitosan coatings can extend the release of protein for longer periods of time. Furthermore, we found that protein molecules are released at faster rates when the temperature of the eluting medium is increased and the pH of the eluting medium is acidic. Nevertheless, it was verified that the release under dynamic conditions is much faster than under static conditions (i.e., about 16 times faster). This can be associated with two main factors: namely; (i) enhanced degradation of chitosan by the action of PBS and (ii) the increment of the diffusion rate of protein molecules from the nanopores to the eluting medium.

CONCLUSIONS

Aluminum wires featuring nanoporous anodic alumina layers produced by electrochemical anodization can be considered as an alternative platform for delivering therapeutics. In this study, for the first time, we have fabricated therapeutic-releasing NAA-Al wires featuring chitosan coatings. The release performance of this platform was systematically studied through a series of in vitro experiments under static and dynamic flow conditions, where the effect of such parameters as the number of chitosan coatings and the pH and temperature of the eluting medium were established. The obtained results revealed that the release of protein molecules under static conditions is much slower than under dynamic flow conditions as a result of two main factors: namely; (i) enhanced degradation of chitosan and (ii) enhancement of diffusion rate of protein molecules from the nanopores to the eluting medium. In addition, we have demonstrated that the release of protein from these platforms is enhanced at acidic pH and higher temperatures.

The combination of nanoengineered aluminum implants with biocompatible and biodegradable polymers such as chitosan can result in many advantages for clinical treatments (e.g., extended release of therapeutics, reduction of side effects associated with toxicity, biointegration, prevention from infections, improved efficiency and efficacy of therapeutics, minimal surgery for implantation, selective targeting of affected tissues/organs, etc.). Undoubtedly, these promising results demonstrate that NAA-Al wires could be a potential platform for future clinical therapies based on localized release of therapeutics. However, more fundamental research and extensive in vitro, ex vivo, and in vivo experiments should be done before this technology becomes reliable and robust.

ASSOCIATED CONTENT

Supporting Information

Further information about TGA analysis of protein-loaded NAA-Al wires, calibration curves used to establish the relationship between fluorescence intensity, absorbance and concentration of BSA-FITC, measurement of chitosan coating thickness by RIfS, and SEM characterization of each fabrication step of NAA-Al wires. This material is available free of charge via the Internet at http://pubs.acs.org.

AUTHOR INFORMATION

Corresponding Authors

*E-mail: abel.santos@adelaide.edu.au. Phone: +61 8 8313 1535. Fax: +61 8 8303 4373. Web page: http://www.adelaide.edu.au/directory/abel.santos.

*E-mail: dusan.losic@adelaide.edu.au. Phone: + 61 8 8313 4648. Fax: +61 8 8303 4373. Web page: http://www.adelaide.edu.au/directory/dusan.losic.

Author Contributions

Dr. Abel Santos designed the experimental part of this study. Cheryl Suwen Law carried out the experiments. The manuscript was written through contributions of all authors. All authors have given approval to the final version of the manuscript.

Notes

The authors declare no competing financial interest.

ACKNOWLEDGMENTS

This research was supported by the Australian Research Council (ARC) through the grants number DE14010054, DP120101680, and FT110100711. Authors thank the School of Chemical Engineering (UoA) and the Adelaide Microscopy (AM) centre for FEG-SEM characterisation.

ABBREVIATIONS

NAA, nanoporous anodic alumina; RIfS, reflection interference spectroscopy; BSA-FITC, bovine serum albumin fluorescein isothiocyanate conjugate

REFERENCES

(1) Langer, R. Drugs on Target. *Science* **2001**, *293*, 58−59.
(2) Blackshear, P. J. Implantable Drug-Delivery Systems. *Sci. Am.* **1979**, *241*, 66−73.
(3) Santos, A.; Sinn Aw, M.; Bariana, M.; Kumeria, T.; Wang, Y.; Losic, D. Drug-Releasing Implants: Current Progress, Challenges and Perspectives. *J. Mater. Chem. B* **2014**, *2*, 6157−6182.
(4) Sinn Aw, M.; Kurian, M.; Losic, D. Non-Eroding Drug-Releasing Implants with Ordered Nanoporous and Nanotubular Structures: Concepts for Controlling Drug Release. *Biomater. Sci.* **2014**, *2*, 10−34.
(5) Sinn Aw, M.; Simovic, S.; Addai-Mensah, J.; Losic, D. Polymeric Micelles in Porous and Nanotube Materials as a New System for Extended Delivery of Poorly Soluble Drugs. *J. Mater. Chem.* **2011**, *21*, 7082−7089.
(6) Sinn Aw, M.; Addai-Mensah, J.; Losic, D. A Multi-Drug Delivery System with Sequential Release Using Titania Nanotube Arrays. *Chem. Commun.* **2012**, *48*, 3348−3350.
(7) Sinn Aw, M.; Addai-Mensah, J.; Losic, D. Polymer Micelles for Delayed Release of Therapeutics from Drug-Releasing Surfaces with Nanotubular Structures. *Macromol. Biosci.* **2012**, *12*, 1048−1052.
(8) Sinn Aw, M.; Addai-Mensah, J.; Losic, D. Magnetic-Responsive Delivery of Drug-Carriers Using Titania Nanotube Arrays. *J. Mater. Chem.* **2012**, *22*, 6561−6563.
(9) Losic, D.; Simovic, S. Self-Ordered Nanopore and Nanotube Platforms for Drug Delivery Applications. *Expert Opin. Drug Delivery* **2009**, *6*, 1363−1381.
(10) Deanesly, R.; Parkes, A. S. Testosterone. *BMJ.* **1936**, *1*, 527−528.
(11) Bishop, P. M. F. A Clinical Experiment in Oestrin Therapy. *BMJ.* **1938**, *1*, 939−941.

DOI: 10.1021/am5091963
ACS Appl. Mater. Interfaces 2015, 7, 3846−3853

(12) Stevenson, C. L.; Santini, J. T., Jr.; Langer, R. Reservoir-Based Drug Delivery Systems Utilizing Microtechnology. *Adv. Drug Delivery Rev.* **2012**, *64*, 1590−1602.
(13) Gulati, K.; Ramakrishnan, S.; Sinn Aw, M.; Atkins, G. J.; Findlay, D. M.; Losic, D. Biocompatible Polymer Coating of Titania Nanotube Arrays for Improved Drug Elution and Osteoblast Adhesion. *Acta Biomater.* **2012**, *8*, 449−456.
(14) Sinn Aw, M.; Khalid, K. A.; Gulati, K.; Atkins, G. J.; Pivonka, P.; Findlay, D.; Losic, D. Characterization of Drug-Release Kinetics in Trabecular Bone from Titania Nanotube Implants. *Int. J. Nanomed.* **2012**, *7*, 4883−4892.
(15) Gulati, K.; Sinn Aw, M.; Losic, D. Nanoengineered Drug-Releasing Ti Wires as an Alternative for Local Delivery of Chemotherapeutics in The Brain. *Int. J. Nanomed.* **2012**, *7*, 2069−2076.
(16) Roy, P.; Berger, S.; Schmuki, P. TiO_2 Nanotubes: Synthesis and Applications. *Angew. Chem., Int. Ed.* **2011**, *50*, 2904−2939.
(17) Kim, G. Y.; Tyler, B. M.; Tupper, M. M.; Karp, J. M.; Langer, R. S.; Brem, H.; Cima, M. J. Resorbable Polymer Microchips Releasing BCNU Inhibit Tumor Growth in The Rat 9L Flank Model. *J. Controlled Release* **2007**, *123*, 172−178.
(18) Grayson, A. C. R.; Choi, I. S.; Tyler, B. M.; Wang, P. P.; Brem, H.; Cima, M. J.; Langer, R. Multi-Pulse Drug Delivery from a Resorbable Polymeric Microchip Device. *Nat. Mater.* **2003**, *2*, 767−772.
(19) Staples, M.; Daniel, K.; Cima, M. J.; Langer, R. Application of Micro- and Nano-Electromechanical Devices to Drug Delivery. *Pharm. Res.* **2006**, *23*, 847−863.
(20) Kam, K. R.; Desai, T. A. Nano- and Microfabrication for Overcoming Drug Delivery Challenges. *J. Mater. Chem. B* **2013**, *1*, 1878−1994.
(21) Albu, S. P.; Ghicov, A.; Aldabergenova, S.; Drechsel, P.; LeClere, D.; Thompson, G. E.; Macak, J. M.; Schmuki, P. Formation of Double-Walled TiO_2 Nanotubes and Robust Anatase Membranes. *Adv. Mater.* **2008**, *20*, 4135−4139.
(22) Kollum, M.; Farb, A.; Schreiber, R.; Terfera, K.; Arab, A.; Geist, A.; Haberstroh, J.; Wnendt, S.; Virmani, R.; Hehrlein, C. Particle Debris from a Nanoporous Stent Coating Obscures Potential Antiproliferative Effects of Tracolimus-Eluting Stents in A Porcine Model of Restenosis. *Catheterization Cardiovasc. Interventions* **2005**, *64*, 85−90.
(23) Masuda, H.; Fukuda, K. Ordered Metal Nanohole Arrays Made by A Two-Step Replication of Honeycomb Structures of Anodic Alumina. *Science* **1995**, *268*, 1466−1468.
(24) Masuda, H.; Hasegwa, F. J. Self-Ordering of Cell Arrangement of Anodic Porous Alumina Formed in Sulfuric Acid Solution. *Electrochem. Soc.* **1997**, *144*, L127−L130.
(25) Masuda, H.; Yada, K.; Osaka, A. Self-Ordering of Cell Configuration of Anodic Porous Alumina with Large-Size Pores in Phosphoric Acid Solution. *Jpn. J. Appl. Phys.* **1998**, *37*, L 1340−L1342.
(26) Nielsch, K.; Choi, J.; Schwirn, K.; Wehspohn, R. B.; Gösele, U. Self-Ordering Regimes of Porous Alumina: The 10% Porosity Rule. *Nano Lett.* **2002**, *2*, 677−680.
(27) Lee, W.; Ji, R.; Gösele, U.; Nielsch, K. Fast Fabrication of Long-Range Ordered Porous Alumina Membranes by Hard Anodization. *Nat. Mater.* **2006**, *5*, 741−747.
(28) Lee, W.; Park, S. J. Porous Anodic Aluminum Oxide: Anodization and Templated Synthesis of Functional Nanostructures. *Chem. Rev.* **2014**, *114*, 7487−7556.
(29) Popat, K. C.; Mor, G.; Grimes, C. A.; Desai, T. A. Surface Modification of Nanoporous Alumina Surfaces with Poly(ethylene glycol). *Langmuir* **2004**, *20*, 8035−8041.
(30) La Flamme, K. E.; Mor, G.; Gong, D.; La Tempa, T.; Fusaro, V. A.; Grimes, C. A.; Desai, T. A. Nanoporous Alumina Capsules for Cellular Macroencapsulation: Transport and Biocompatibility. *Diabetes Technol. Ther.* **2005**, *7*, 684−694.
(31) La Flamme, K. E.; Popat, K. C.; Leoni, L.; Markiewicz, E.; La Tempa, T. J.; Roman, B. B.; Grimes, C. A.; Desai, T. A. Biocompatibility of Nanoporous Alumina Membranes for Immunoisolation. *Biomaterials* **2007**, *28*, 2638−2645.
(32) Wang, Y.; Santos, A.; Kaur, G.; Evdokiou, A.; Losic, D. Structurally Engineered Anodic Alumina Nanotubes as New Nano-Carriers for Delivery of Anticancer Therapeutics. *Biomaterials* **2014**, *35*, 5517−5526.
(33) Simovic, S.; Losic, D.; Vasilev, K. Controlled Drug Release form Porous Materials by Plasma Polymer Deposition. *Chem. Commun.* **2010**, *46*, 1317−1319.
(34) Kumeria, T.; Gulati, K.; Santos, A.; Losic, D. Real-Time and In Situ Drug Release Monitoring from Nanoporous Anodic Alumina Under Dynamic Flow Conditions by Reflectometric Interference Spectroscopy. *ACS Appl. Mater. Interfaces* **2013**, *5*, 5436−5442.
(35) Tahvanainen, M.; Rotko, T.; Mäkilä, E.; Santos, H. A.; Neves, D.; Laaksonen, T.; Kallonen, A.; Hämäläinen, K.; Peura, M.; Serimaa, R.; Salonen, J.; Hirvonen, J.; Peltonen, L. Tablet Preformulations of Indomethacin-Loaded Mesoporous Silicon Microparticles. *Int. J. Pharm.* **2012**, *422*, 125−131.
(36) Gibaldi, M.; Feldman, S. Establishment of Sink Conditions in Dissolution Rate Determinations: Theoretical Considerations and Application to Nondisintegrating Dosage Forms. *J. Pharm. Sci.* **1967**, *56*, 1238−1242.
(37) Champagne, M.; Luzzati, V.; Nicolaieff, A. The Size and Shape of Bovine Serum Albumin as A Function of pH, Determined by Small-Angle Scattering of X-Rays. *J. Am. Chem. Soc.* **1958**, *80*, 1002−1003.
(38) Santos, A.; Balderrama, V. S.; Alba, M.; Formentín, P.; Ferré-Borrull, J.; Pallarès, J.; Marsal, L. F. Nanoporous Anodic Alumina Barcodes: Toward Smart Optical Biosensors. *Adv. Mater.* **2012**, *24*, 1050−1054.
(39) Santos, A.; Kumeria, T.; Losic, D. Optically Optimized Photoluminescent and Interferometric Biosensors based on Nanoporous Anodic Alumina: A Comparison. *Anal. Chem.* **2013**, *85*, 7904−7911.
(40) Santos, A.; Kumeria, T.; Losic, D. Nanoporous Anodic Aluminum Oxide for Chemical Sensing and Biosensors. *TrAC, Trends Anal. Chem.* **2013**, *44*, 25−38.
(41) Santos, A.; Kumeria, T.; Wang, Y.; Losic, D. In Situ Monitored Engineering of Inverted Nanoporous Anodic Alumina Funnels: On the Precise Generation of 3D Optical Nanostructures. *Nanoscale* **2014**, *6*, 9991−9999.
(42) Gulati, K.; Sinn Aw, M.; Losic, D. Drug-Eluting Ti Wires with Titania Nanotube Arrays for Bone Fixation and Reduced Bone Infection. *Nanoscale Res. Lett.* **2011**, *6*, 1−6.
(43) Pillai, C. K. S.; Paul, W.; Sharma, C. P. Chitin and Chitosan Polymers: Chemistry, Solubility and Fiber Formation. *Prog. Polym. Sci.* **2009**, *34*, 641−678.
(44) Ford, J. L.; Mitchell, K.; Rowe, P.; Armstrong, D. J.; Elliott, P. N. C.; Rostron, C.; Hogan, J. E. Mathematical Modelling of Drug Release from Hydroxypropylmethylcellulose Matrices: Effect of Temperature. *Int. J. Pharm.* **1991**, *71*, 95−104.

DOI: 10.1021/am5091963
ACS Appl. Mater. Interfaces 2015, 7, 3846−3853